JOURNAL OF MATERIALS SCIENCE 32 (1997) 3163–3175

In situ microscopy of crack healing in borosilicate glass

B. A. WILSON, E. D. CASE
Department of Materials Science and Mechanics, Michigan State University, East Lansing, MI 48824, USA

In situ environmental scanning electron microscopy studies of semi-macro indent cracks in borosilicate glass indicate that crack healing occurred at humidities as low as 8% relative humidity and at temperatures as low as about 400 °C. The crack morphology changes observed *in situ* include slow crack regression (at low temperatures) and multiple crack pinch-off (at higher temperatures). Subsurface crack morphology changes were observed using conventional scanning electron microscopy of the fractured healed specimens. Subsurface healing included pinch-off into voids which appear quasi-circular in cross-section. In addition, crack debris were observed to hinder the crack healing process, which has important implications for fatigue of ceramic materials, where debris generation is frequently reported in the literature.

1. Introduction

1.1. Crack healing in ceramics

Crack healing has been observed in a variety of different ceramic materials including single crystals [1–3], polycrystalline ceramics [2,4, 5], inorganic glasses [6, 7] and ceramic composites [8]. Three general mechanisms have been reported for crack healing in ceramics: diffusion-driven thermal healing, adhesion from intermolecular forces and reaction products from chemical reactions at the crack tip [4].

Thermal-annealing induced changes in crack morphology have been treated theoretically by Nichols [9] and Nichols and Mullins [10]. They [9, 10] showed that a semi-infinite cylindrical crack would either evolve (by diffusive transport) into a string of small spherical pores (ovulation) or into a large sphere (spheroidization).

Experimental observations of crack morphology changes [1–3, 5] are consistent with Nichols and Mullins' theoretical observations [9, 10]. For example, Yen and Coble [3] thermally annealed internal cracks in single crystal sapphire in air at temperatures ranging from 1650 to 1810 °C. They found that the original continuous internal cracks broke up into channels of tubular voids which evolved into rows of spherical pores. Wang *et al.* [1] used an *in situ* optical microscope to observe healing of internal cracks in single crystal LiF during isothermal annealing in the temperature range of 620 to 820 °C. The thermal annealing occurred in three stages: pinching off of plane cracks into cylindrical pores, ovulation of cylindrical pores and shrinkage of isolated pores. Gupta [2, 5] investigated healing in MgO, sapphire and alumina. Cracks formed from thermal down-shocking were thermally annealed at temperatures in the 1400 to 1700 °C range. The specimens were annealed, fractured in four-point bend, and observed in an SEM. Gupta observed pinching off of the cracks at grain boundaries (for MgO and alumina) and that the cracks evolved into cylindrical voids. The cylindrical voids became rows of spherical pores and with further annealing the spherical pores underwent continuous shrinkage.

Crack healing studies in inorganic glasses have frequently emphasized the role of environmental humidity in the crack healing process. Holden and Frechette [6] studied the thermal annealing of soda-lime silica glass specimens containing cracks formed from thermal down-shock by a metal probe. The specimens were annealed at 550 °C in a humid environment and then fractured using a ring-on-ring test. Fracture surfaces were observed using differential interference contrast. Based on their results, Holden and Frechette [6] proposed a four step model for the crack healing in soda-lime silica glass: adsorption of water at a temperature below the glass transition temperature, formation of a gel layer, closure of the crack due to stress relief and drying of the gel in the presence of a controlled atmosphere.

Using an optical microscope, Lehman *et al.* [7] healed Vickers indentation cracks in fluoride glass under different relative humidity levels at temperatures of 22, 50 and 80 °C. The crack closure rate was greater at higher levels of relative humidity, while crack closure lengths appear to reach similar values at longer times for all levels of humidity. Lehman *et al.* [7] found no evidence of a gel or any other reaction product which they state would be crystalline in fluoride glass and readily identifiable.

This study employs an environmental scanning electron microscope (ESEM) to observe crack healing in a borosilicate glass. The ESEM, equipped with a hot

0022–2461

stage, allowed one to directly examine crack healing under a range of humidity conditions and at elevated temperatures. Pinch-off and regression of the surface trace of the indentation cracks were observed *in situ* in the ESEM, while the subsurface changes in crack morphology were inferred via a conventional scanning electron microscopy (SEM) study on specimens which were first thermally annealed and then fractured through the partially-healed indentation cracks. Also, *in situ* ESEM observation revealed that debris in the crack inhibited healing. Since mechanical fatigue in ceramics can produce a significant amount of debris [11], the interaction of debris and the crack healing process is potentially very important to the high temperature behaviour of mechanically fatigued ceramics.

1.2. ESEM capabilities

Conventional scanning electron microscopes (SEM) use electrons to form an image of a specimen's surface. The Everhart–Thornley detector collects secondary electrons (SE) and back scattered electrons (BSE) generated from interactions between the incident electrons and the surface [12]. The specimen chamber in an SEM must remain under vacuum for an image to be formed by using the Everhart–Thornley detector [12].

An environmental scanning electron microscope (ESEM) also uses electrons to form an image of a specimen's surface. However, the ESEM uses a gaseous detection device (GDD) to collect SE and BSE electrons and thus the sample chamber in an ESEM allows the presence of a gaseous environment around the sample [13]. The ESEM has a number of pressure levels along the path of the electron beam. The differing pressure levels are separated by pressure limiting apertures (PLA) which allow the electron gun to be under high vacuum while the specimen chamber can be pressurized up to 3.33×10^3 Pa [13]. The GDD operates with a positive bias of a few hundred volts. SE emitted from the sample surface are accelerated toward the detector. Along the way the SE collide with gas molecules, which eject electrons from the gas molecules. This process is repeated and results in an avalanche process [13] which amplifies the SE signal. The process of electron ejection from gas molecules creates positive gas ions which help neutralize the buildup of a negative charge on the sample surface and allows the use of non-conducting samples without a conductive coating [12]. Danilatos [13] has shown no loss of resolution using the GDD detector in a gaseous environment compared to using an Everhart–Thornley detector at high vaccum.

The unique capabilities of the ESEM allowed this *in situ* study of the crack healing of ceramics. The ability to have a gaseous environment in the specimen chamber allowed the crack healing specimens to initially be in a humid environment. (As the temperature increases the relative humidity drops rapidly. At temperatures above 100 °C, the relative humidity at pressures below 1330 Pa becomes negligibly small [13].) Also, the ESEM can examine ceramic specimens without the conductive coating required for a conventional SEM. The elimination of the conductive surface coating avoids contamination and other perturbations of the crack healing process that might stem from heating the specimen with a surface coating in place. The absence of the surface coating also allows a more direct, unobstructed observation of the surface trace of the cracks during the healing process.

2. Experimental procedure

2.1. ESEM investigations

Using a low speed diamond saw, the specimens used for the ESEM study were cut from 1.1 mm thick commercially available glass slides (Fisher Scientific Microscope Slides). The edges of the 4 mm by 4 mm specimens were polished and the four corners were slightly rounded using 240, 320, 400 and 600 grit SiC fixed-abrasive paper. A Vickers indent was placed in the centre of a 4 mm by 4 mm specimen face with a load of 9.8 N applied by a commercial hardness tester (Buehler Semimacro Hardness Tester). The specimens were then aged for at least 24 h.

The glass specimens were tested in an ESEM (Electroscan Model 2020 ESEM) with a hot stage capable of temperatures up to 1000 °C. Once the specimens were loaded in the ESEM the initial relative humidity was set by the temperature in the laboratory and by the pressure in the ESEM sample chamber. Micrographs of the initial indent cracks were taken before the specimen was heated. The heated schedule was selected by specifying up to five sets of temperature set point, ramp rate and dwell time data. Once heating began, micrographs of the indent cracks were taken at selected times and temperatures.

2.2. Conventional SEM investigations

The subsurface crack healing behaviour for borosilicate glass was investigated by first thermally annealing Vickers indentation cracks in specimens, then fracturing the specimens through the partially healed indent cracks to observe the partially healed Vickers cracks in a conventional SEM. A high speed diamond saw cut the 11 mm by 76 mm specimens from the 1.1 mm thick borosilicate glass. The edges of the specimens were rounded as described for the ESEM samples. Using a 9.8 N load, a Vickers indent was centred on the 11 mm by 76 mm surface. The initial indent crack lengths were measured more than 24 h after the indents were made to allow for a saturation in slow crack growth and therefore a stabilization in the crack lengths.

The samples were heated in a tube furnace at 10 °C min^{-1} to a set temperature of 550 °C, held for 30 min and cooled at 10 °C min^{-1} to 450 °C. From 450 °C to room temperature, the furnace cooled freely. The thermally annealed samples and the non-heat-treated samples were all fractured. The failure surface of thermally annealed and non-heat-treated specimens were observed in an SEM (Jeol JSM-6400V).

The specimens were fractured using a technique (originally developed by Kirchner [14]) which seeks to minimize subcritical extension of the crack under

study. A series of four to six 9.8 N indents placed on the specimen face opposite the partially healed indentation crack were aligned with the partially healed indent crack by focusing through the specimen. From four to eight 49 N indents (collinear with the 9.8 N indents) lead to crack coalescence and catastrophic failure. Kirchner's [14] technique thus avoided a subcritical crack extension of the partially healed indentation crack by avoiding direct loading on the partially healed crack.

3. Results and discussion

3.1. *In situ ESEM*

Four different experiments were performed and are labelled as alpha, beta, gamma and delta for this discussion. The heating schedules for experiments alpha–delta are given in Tables I–IV, respectively.

The specimen in experiment alpha was initially held in the ESEM chamber at 25 °C and a water vapour pressure of 333 Pa, which corresponds to 10% relative humidity (see Appendix in [13]). Before heating, the average indentation crack length was 181 μm (Fig. 1). Upon heating (Table I), when the specimen first reached

TABLE I ESEM hot stage heating schedule for specimen in experiment alpha

	Set point (°C)	Ramp rate (°C min^{-1})	Dwell time (min)
1	300	20	5
2	400	20	10
3	500	10	20
4	550	5	30
5	600	2	135

TABLE II ESEM hot stage heating schedule for specimen in experiment beta

	Set point (°C)	Ramp rate (°C min^{-1})	Dwell time (min)
1	400	20	10
2	430	5	35
3	450	1	10
4	470	1	10
5	490	1	40

TABLE III ESEM hot stage heating schedule for specimen in experiment gama

	Set point (°C)	Ramp rate (°C min^{-1})	Dwell time (min)
1	370	20	15
2	430	5	15
3	25[a]	20[a]	[a]
4	370	20	15
5	430	10	175

[a]ESEM shut down, so specimen was cooled to room temperature and the ESEM was rebooted.

TABLE IV ESEM hot stage heating schedule for specimen in experiment delta

	Set point (°C)	Ramp rate (°C min^{-1})	Dwell time (min)
1	400	20	1
2	500	10	30
3	550	5	110
4	560	1	15
5	575	1	35
6	600	1	30
7	610	1	10

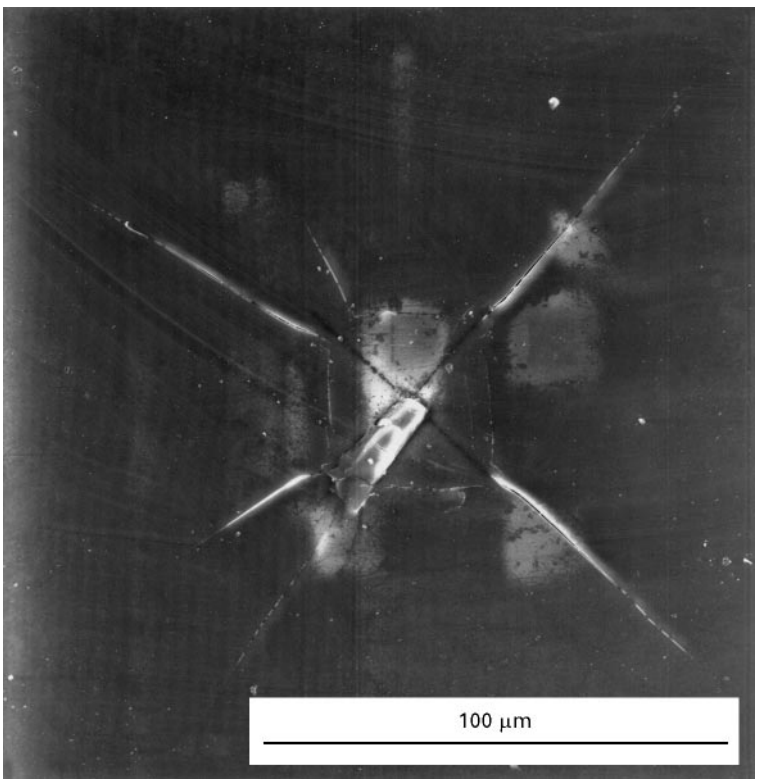

Figure 1 Micrograph of indention cracks of borosilicate glass specimen (experiment alpha) at 25 °C and 10% relative humidity.

600 °C, the average indentation crack length had decreased to 96 μm, a decrease of about 47 per cent from the initial crack length (Fig. 2). After the specimen was held at 600 °C for 38 min, multiple areas of crack pinch-off were evident along the length of the crack (Fig. 3). During the 38 min at 600 °C, the crack length decreased by 30%.

In experiment beta, the specimen was initially held in the ESEM chamber at 27 °C and a water vapour pressure of 1280 Pa (8% relative humidity) and was

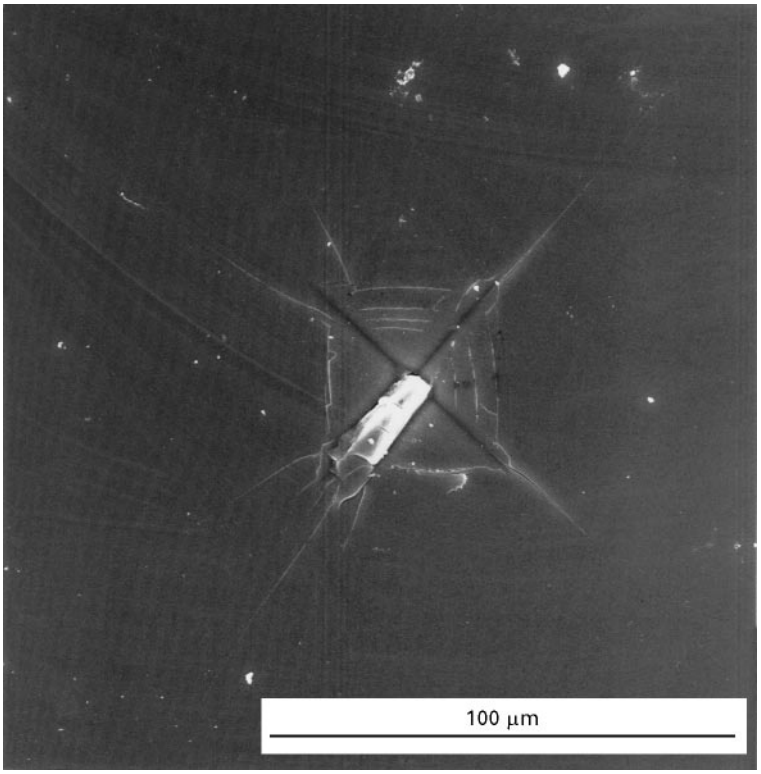

Figure 2 Micrograph of borosilicate glass specimen (experiment alpha) upon reaching 600 °C exhibiting crack healing. The same indentation crack system prior to healing, is shown in Fig. 1.

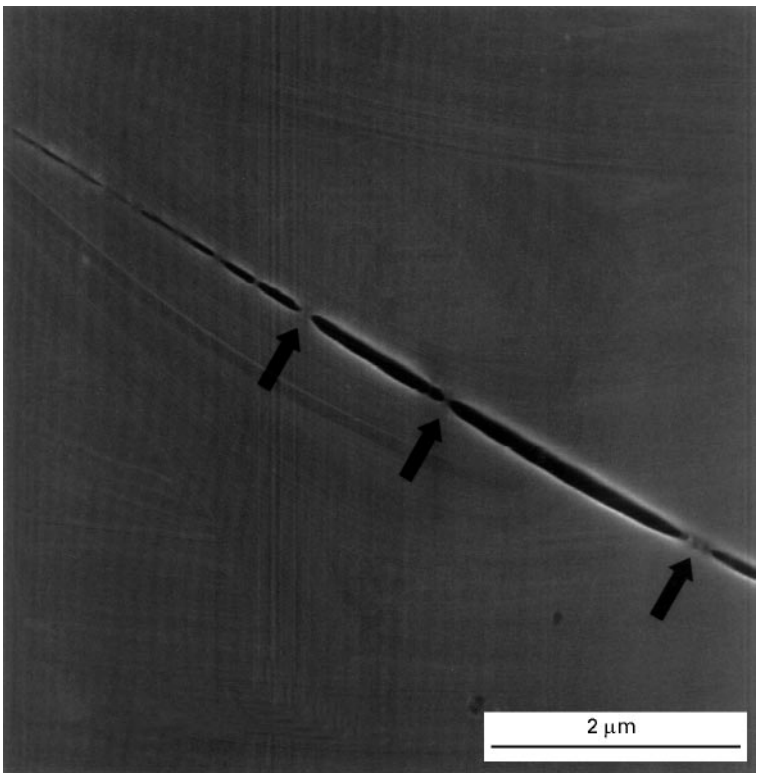

Figure 3 Micrograph of borosilicate glass specimen (experiment alpha) 38 min after reaching 600 °C showing multiple crack pinch-off (arrows show some pinch-off areas).

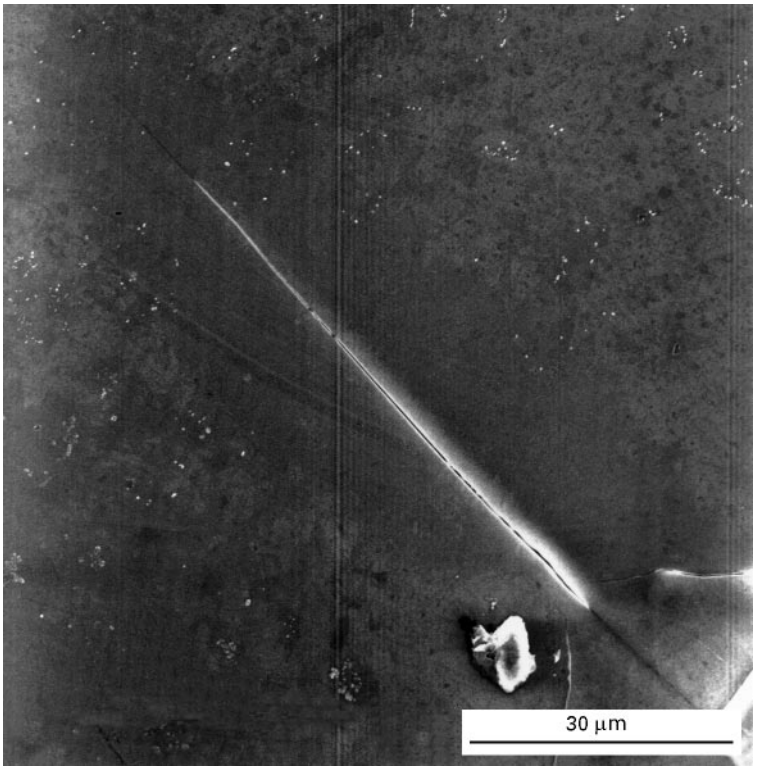

Figure 4 Micrograph of indention cracks of borosilicate glass specimen (experiment beta) at 27 °C and 8% relative humidity.

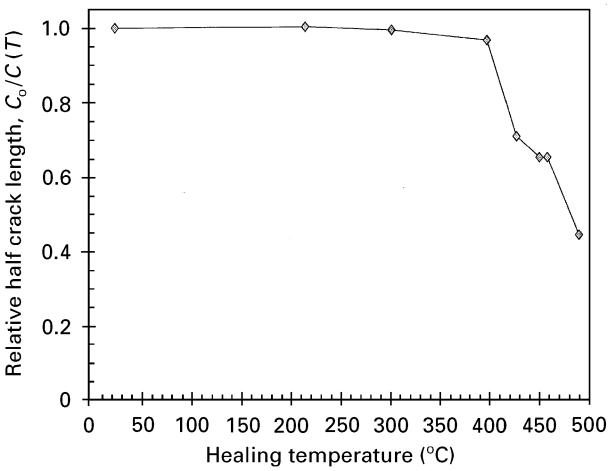

Figure 5 Decrease in the crack length of a borosilicate glass specimen (experiment beta) in the ESEM as a function of hot stage temperature for experiment beta. The time at each temperature is given in Table II.

thermally annealed at temperatures up to 490 °C (Table II). Experiment beta revealed crack healing at lower initial relative humidity levels and lower temperatures than in experiment alpha. The initial half crack length was 105 μm (Fig. 4). A small amount of crack healing commenced before the isothermal hold at 430 °C (Fig. 5). After 10 min at 430 °C, the half crack length was reduced by 30% (Fig. 5). Approximately 8 min after the specimen reached 490 °C (Fig. 6), the crack length decreased to 46 μm (a 55% reduction in crack length compared to the initial crack length).

In experiment gamma (an isothermal hold at 430 °C), the specimen was initially held in the ESEM chamber at 21 °C and a water vapour pressure of 320 Pa (14% relative humidity). During thermal annealing (Table III), the crack length initially decreased rapidly but the rate of change of crack length decreased over time (Figs 7–9).

In experiment delta, the glass specimen was initially held in the ESEM chamber at 25 °C and a water vapour pressure of 333 Pa (10% relative humidity). Experiment delta (Table IV) demonstrated the interaction between a piece of crack debris and the healing process (Figs 10–13). Figs 11–13 depict, respectively, a close up of the region of the crack with the debris after 30 min at 575 °C, the same region after 5 min at 600 °C, and the crack morphology immediately after reaching 610 °C for a similar field of view as Fig. 10.

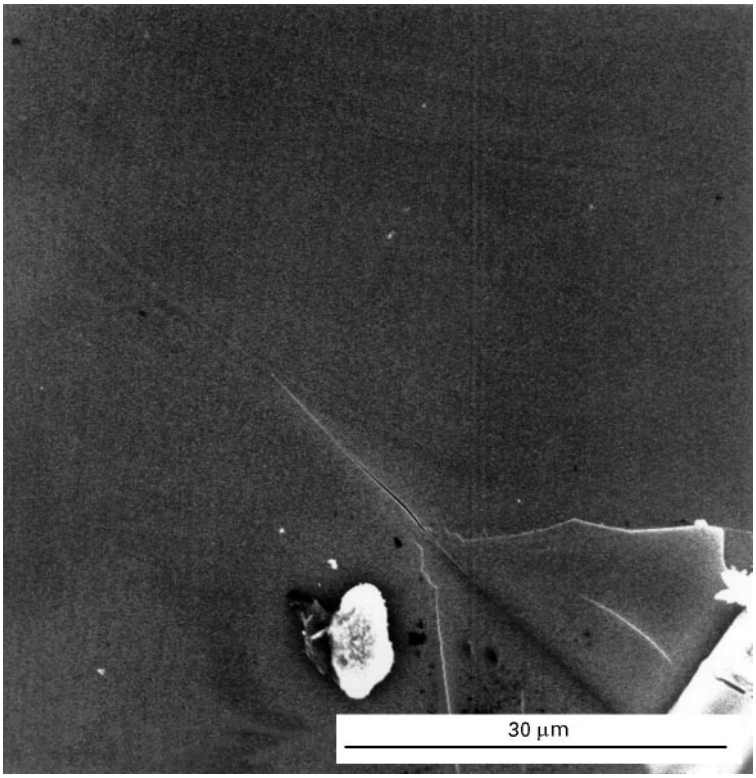

Figure 6 Micrograph of borosilicate glass specimen (experiment beta) after 8 min at 490 °C exhibiting crack healing.

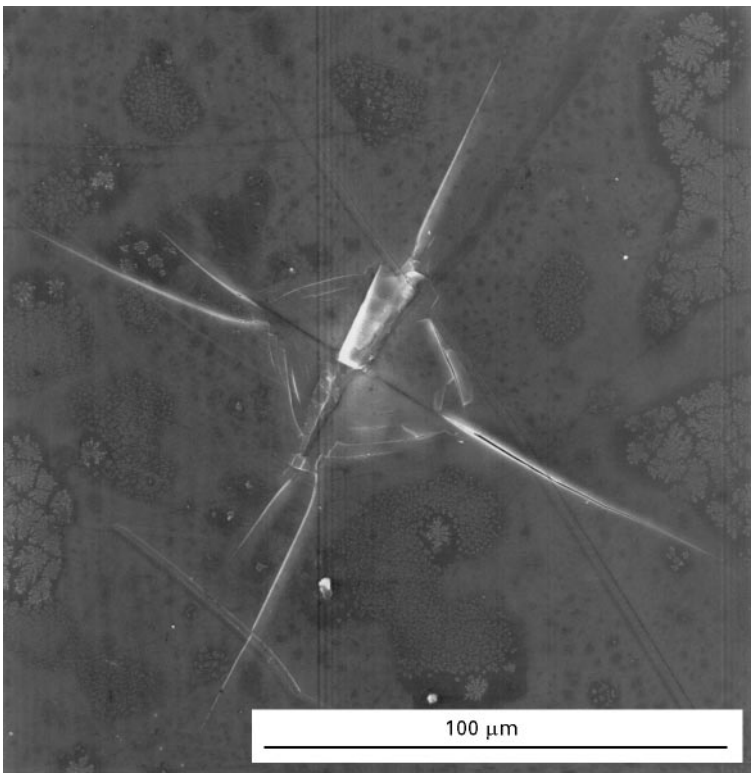

Figure 7 Micrograph of indention cracks of borosilicate glass specimen (experiment gama) at 21 °C and 14% relative humidity.

At 550 °C for experiment delta, the debris can be seen in a portion of a pinched-off crack (the debris is indicated by an arrow in Figs 10 and 14). Note that Vickers indentation crack systems typically include four radial cracks (Figs 1 and 7). For each of the radial cracks in each of the four specimens (in experiments alpha, beta, gamma and delta), healing progressed from the crack tip toward the indent impression

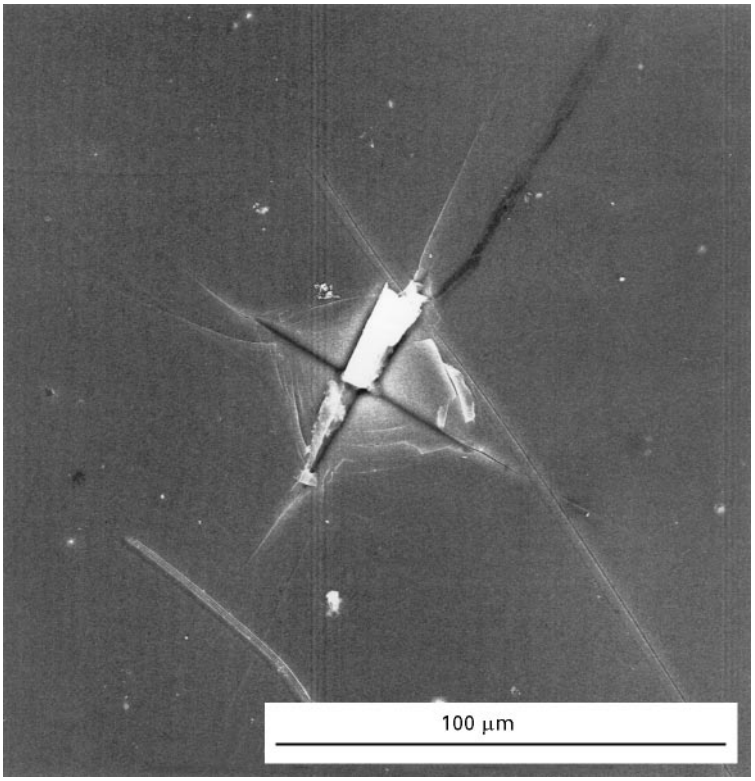

Figure 8 Micrograph of borosilicate glass healing specimen (experiment gama) after 110 min at 430 °C.

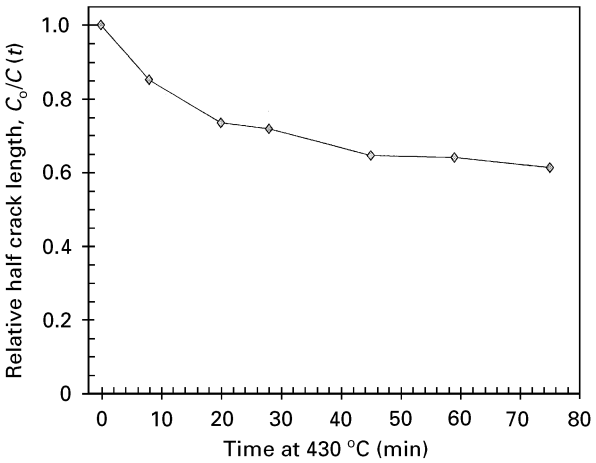

Figure 9 Decrease in the crack length of a borosilicate glass specimen (experiment gama) in the ESEM as a function of the time held at 430 °C for experiment gamma.

(Fig. 15), except for the one radial crack containing the debris in experiment delta (Figs 10–13). For the radial crack that contained the debris, initially crack regression from the crack tip and crack pinch-off occurred (Fig. 10), as was the case for the other cracks (without debris) in this study (Fig. 15). However, as the crack morphology changes associated with healing reached the debris site (Fig. 11), the crack healing process changed. In the vicinity of the debris, the crack is wedged open apparently without healing (Fig. 12). The crack then began to regress toward the debris from the end of the crack near the indent impression. Also, the crack pinched-off between the debris and the nascent crack tip (Figs 13 and 15). In the area near the debris, complete healing still has not occured (Fig. 13). The impediment of crack healing by debris within the crack could adversely effect the healing of ceramics which have undergone mechanical fatigue since debris has been reported to be produced during the mechanical fatigue of ceramics [11].

The ESEM micrographs depict only the specimen surface and so it is unclear if the cracks below the specimen surface break into cylindrical voids and/or break into spheres as seen in internal cracks by Gupta [2, 5] and Wang *et al.* [1]. To investigate the crack

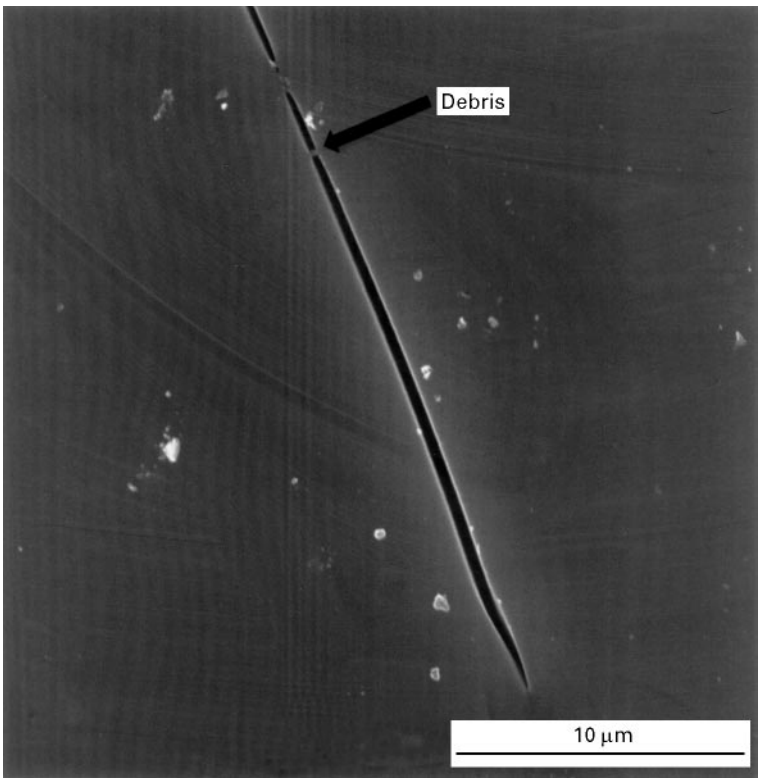

Figure 10 ESEM micrograph of borosilicate glass specimen (experiment delta) at 550 °C showing pinch-off and location of debris (arrow).

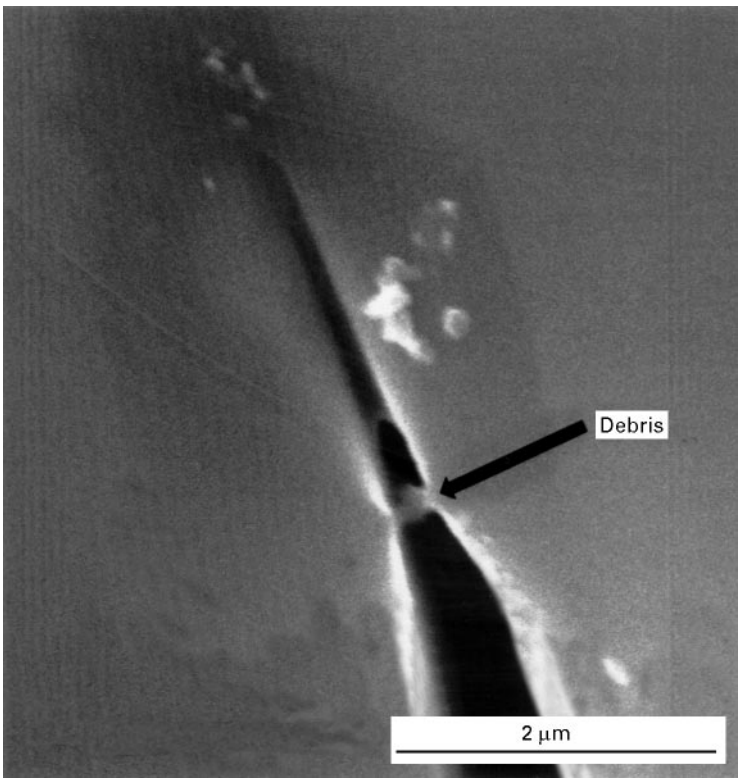

Figure 11 ESEM micrograph of borosilicate glass specimen (experiment delta) at 575 °C showing close up of area near debris (arrow) and crack healing approaching the debris.

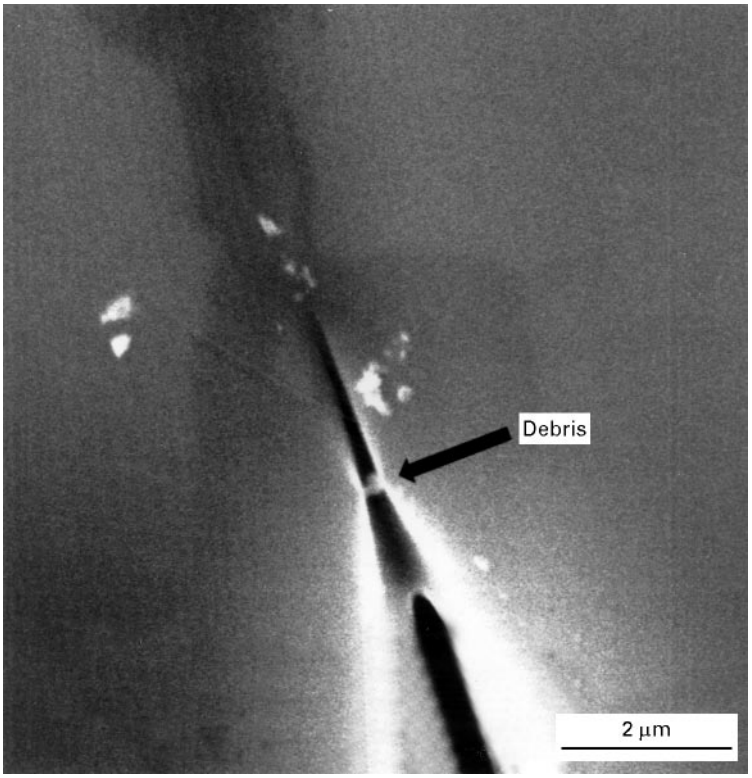

Figure 12 ESEM micrograph of borosilicate glass specimen (experiment delta) at 600 °C showing close up area near debris (arrow) and crack healing passing the debris without complete healing.

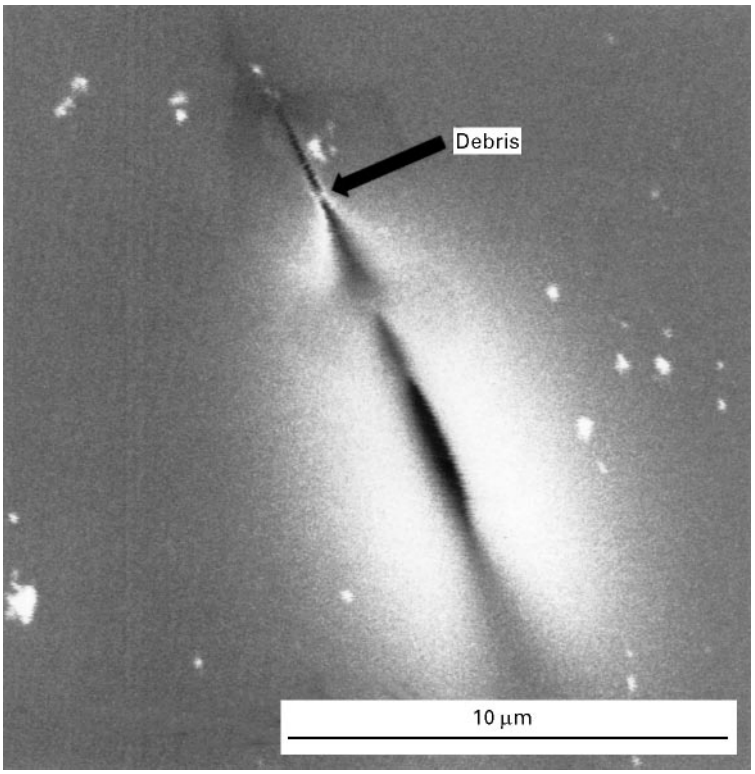

Figure 13 ESEM micrograph of borosilicate glass specimen (experiment delta) at 610 °C showing healing from bottom part of the crack approaching the debris (arrow) without complete healing in the area of the debris.

healing below the surface, conventional scanning electron microscopy was done on thermally annealed borosilicate specimens that were fractured using Kirchner's technique [14].

3.2. Conventional SEM

The relative crack lengths (C_i/C_f) after heat treatment at 550 °C for 30 min are shown in Table V. Each crack observed using an optical microscope had a heavy and

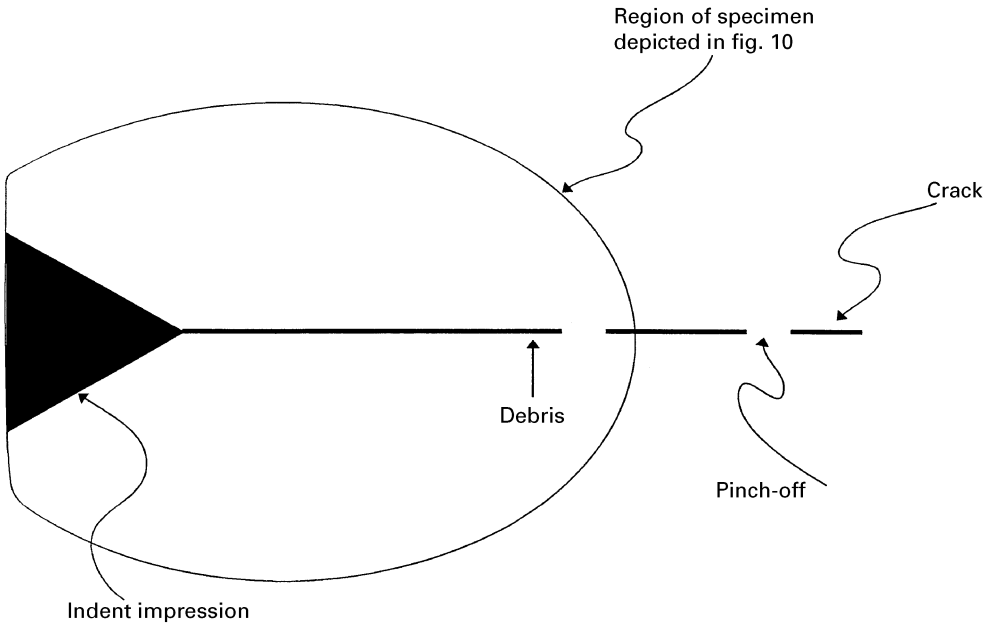

Figure 14 Schematic of half of the indent crack of the borosilicate glass specimen from experiment delta after 20 min at 550 °C (Table IV). Included in the schematic are: the region of the specimen depicted in Fig. 10, multiple crack pinch-off, and the location of the debris.

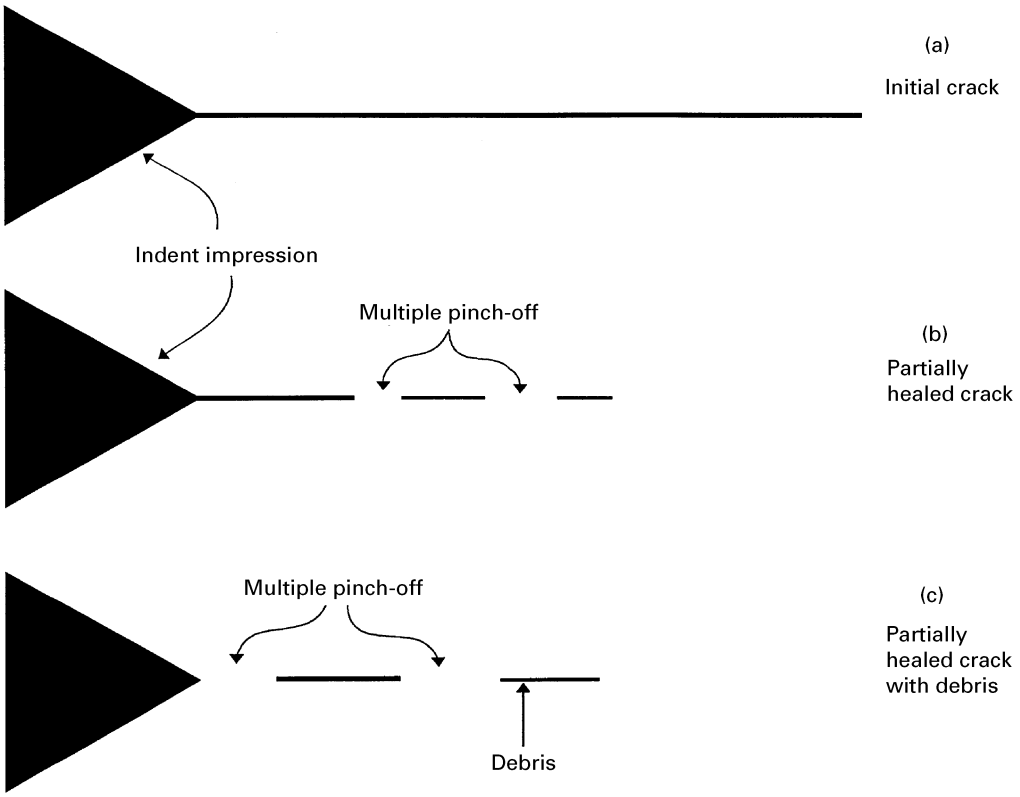

Figure 15 (a) Schematic of half of an initial Vickers indentation crack (before heat treatment), (b) schematic of a partially healed indentation crack showing the typical regression of the crack from the tip toward the indent impression, and (c) schematic of a partially healed indentation crack containing debris (experiment delta) that includes crack regression toward the debris from the end of the crack near the indent impression.

faint portion. The heavy portion of the crack was characterized by a large crack opening displacement with a rounded crack tip. The faint portion of the crack extended from the end of the heavy portion of the crack and had negligible crack opening displacement.

Specimen 5B550 was fractured through the partially healed indent crack and observed in the conventional SEM. Fig. 16a is a conventional SEM micrograph of half of the heat-treated, subsurface indent crack. Fig. 16b and c are higher magnification micrographs of the upper right hand region of the crack in Fig. 16a.

The ESEM micrographs depict only the specimen surface and so ESEM observations alone cannot determine if the cracks below the specimen surface break into cylindrical voids and/or break into spheres as seen in internal cracks by Wang *et al.* [1], Gupta [2, 5] and Yen and Coble [3]. To investigate the crack healing below the surface, conventional scanning electron microscopy was done on thermally annealed borosilicate specimens. A line of voids that appear quasi-circular in cross-section was observed for a borosilicate glass specimen partially healed by a 30 min heat treatment at 550 °C (specimen 5B550 Table V, Fig. 16). While this phenomenon needs to be investigated further, the appearance of the voids seems

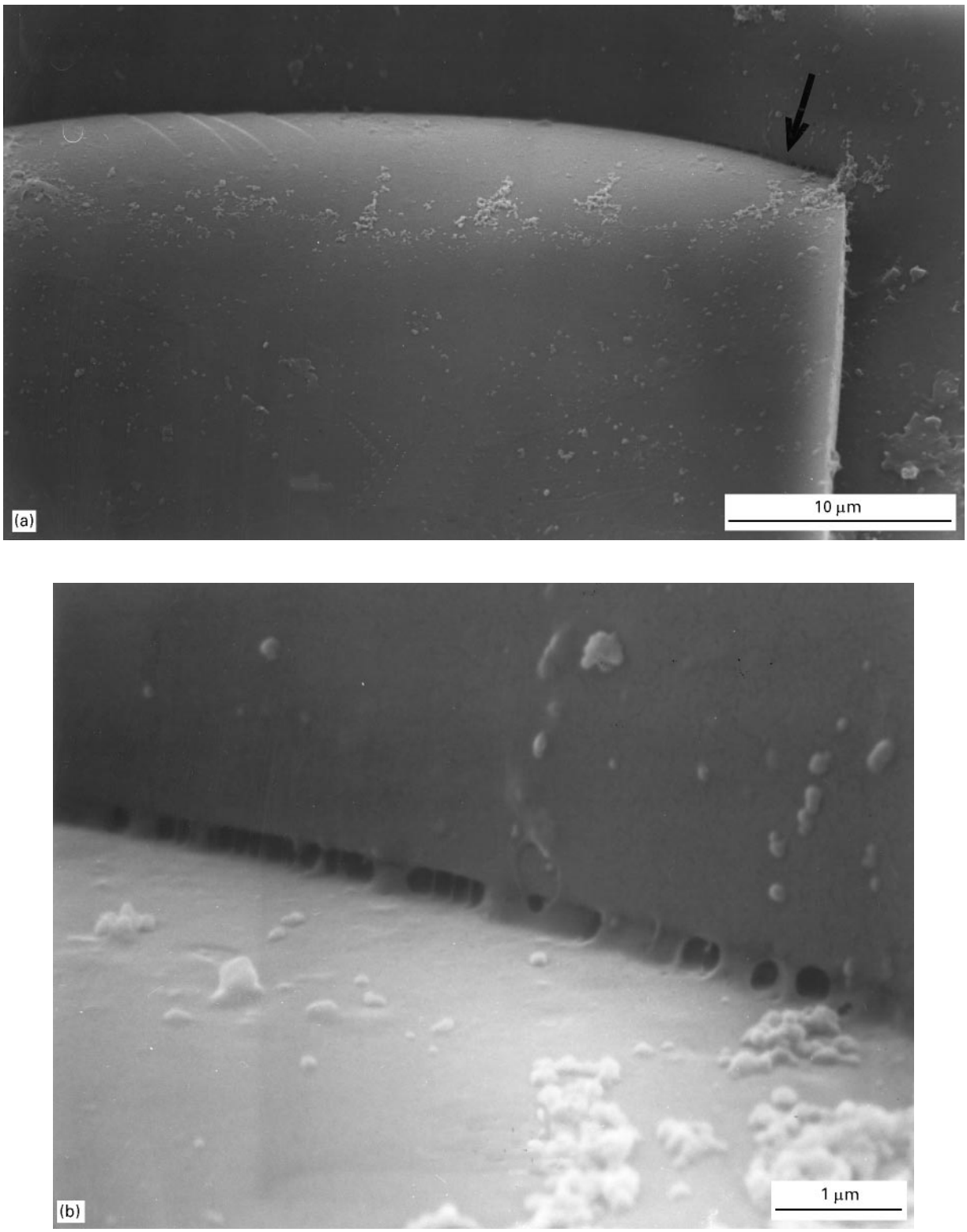

Figure 16 Conventional SEM micrograph of fracture surface of a partially healed borosilicate glass specimen (specimen 5B550 in Table V) heat treated for 30 min at 550 °C. (a) Subsurface portion of Vickers indent at 2.500×, (arrow indicates region of quasi-circular voids), (b) region of quasi-circular voids at 15 000×, (c) region of quasi-circular voids at 30 000×.

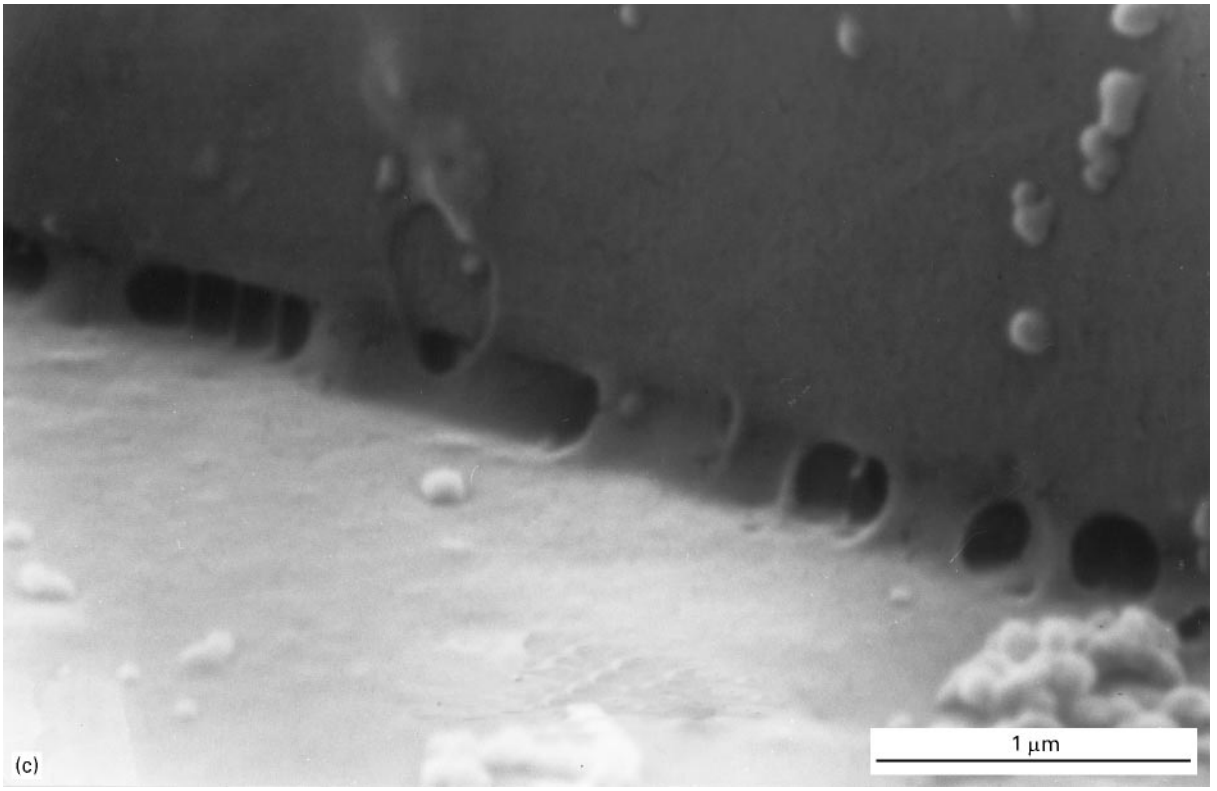

Figure 16 Continued.

TABLE V Relative crack lengths measured via an optical microscope for borosilicate glass specimens after heat treatment in a tube furnace at 550 °C for 30 min

Specimen	Relative crack length (faint)		Relative crack length (heavy)	
	$2c_1$	$2c_2$	$2c_1$	$2c_2$
1B550	0.970	0.914	0.694	0.621
2B550	0.988	0.849	0.908	0.792
3B550	0.930	0.892	0.843	0.845
4B550	0.789	0.773	0.723	0.696
5B550	0.971	0.973	0.723	0.633

indicative of the appearance of the type of crack healing and pinch-off discussed by previous researchers [1–3, 5].

4. Summary and conclusions

In situ electron microscopy was used to observe healing of semi-macro indent cracks in borosilicate glass in a humid environment using an environmental scanning electron microscope. Crack healing occurred at initial humidities as low as 8% and at temperatures as low as about 400 °C. In the absence of debris wedged within the crack, healing began at the crack tip and moved toward the indent impression (Figs 2, 5 and 8). Multiple crack pinch-off was observed as a mechanism of crack healing at temperatures above 500 °C. Figs 3, 10, 11, 12 and 13 show changing crack morphology rather than a simple closing of the crack indicating that the likely healing mechanism was not adhesion due to intermolecular forces [4, 6]. Crack pinch-off behaviour observed in the borosilicate glass (Fig. 3) was similar to that seen in other ceramic materials by other investigators [1, 2, 5].

Fig. 3 does not show the evenly spaced pinch-off proposed by Nichols and co-worker [9, 10] and observed by other investigators [1, 2, 5]. The uneven spacing between crack pinch-off locations may be related to the increase in crack opening displacement along the length of the crack as one proceeds from the crack tip to the indent impression. As the crack opening displacement along the crack increases (lower right hand portion of the figure), the distance between crack pinch-off locations also increases (Fig. 3).

Conventional SEM microscopy of the partially healed fracture surface revealed subsurface crack morphology changes similar in appearance to crack morphology changes reported in the literature [1–3, 5].

Debris in a crack was observed to hinder complete crack healing. The interaction between crack surface debris and the crack healing process implies that ceramic materials which have been mechanically fatigued could have healing impeded by the debris formed during cycling.

Acknowledgements

The authors would like to acknowledge the financial support of the Research Excellence Fund of the State of Michigan. Also, we would like to thank Steve Roseveld and the Composite Materials and Structures Center (CMSC) at Michigan State University for the use of the ESEM.

References

1. Z. WANG, Y. Z. LI, M. P. HARMER and Y. T. CHOU, *J. Amer. Ceram. Soc.* **75** (1992) 1596.
2. T. K. GUPTA, *ibid.* **59** (1976) 259.
3. C. F. YEN and R. L. COBLE, *ibid.* **55** (1972) 507.
4. E. D. CASE, J. R. SMYTH and O. HUNTER JR, in "*Fracture Mechanics of Ceramics*", Vol. 5 (Plenum Press, New York, 1983) pp. 507–530.
5. T. K. GUPTA, *J. Amer. Ceram. Soc.* **58** (1975) 143.
6. M. K. C. HOLDEN and V. D. FRECHETTE, *ibid.* **72** (1989) 2189.
7. R. L. LEHMAN, R. E. HILL JR and G. H. SIGEL JR, *ibid.* **72** (1989) 474.
8. A. M. THOMPSON, H. M. CHAN, M. P. HARMER and R. F. COOK, *ibid.* **78** (1995) 567.
9. F. A. NICHOLS, *J. Mater. Sci.* **11** (1976) 1077.
10. F. A. NICHOLS and W. W. MULLINS, *Trans. Met. Soc. AIME* **233** (1965) 1840.
11. L. EWART and S. SURESH, *J. Mater. Sci.* **22** (1987) 1173.
12. S. F. FLEGLER, J. W. HECKMAN JR and K. L. KLOMPARENS, "Scanning and Transmission Electron Microscopy: An Introduction" (W. H. Freeman and Company, New York, 1993).
13. G. D. DANILATOS, *Microsc. Res. Tech.* **25** (1993) 354.
14. H. P. KIRCHNER, *J. Amer. Ceram. Soc.* **67** (1984) 127.

Received 13 May
and accepted 23 October 1996